JOURNAL OF GEOPHYSICAL RESEARCH, VOL. 102, NO. B3, PAGES 5005–5017, MARCH 10, 1997

Precise point positioning for the efficient and robust analysis of GPS data from large networks

J. F. Zumberge, M. B. Heflin, D. C. Jefferson, M. M. Watkins, and F. H. Webb
Jet Propulsion Laboratory, California Institute of Technology, Pasadena

Abstract. Networks of dozens to hundreds of permanently operating precision Global Positioning System (GPS) receivers are emerging at spatial scales that range from 10^0 to 10^3 km. To keep the computational burden associated with the analysis of such data economically feasible, one approach is to first determine precise GPS satellite positions and clock corrections from a globally distributed network of GPS receivers. Then, data from the local network are analyzed by estimating receiver-specific parameters with receiver-specific data; satellite parameters are held fixed at their values determined in the global solution. This "precise point positioning" allows analysis of data from hundreds to thousands of sites every day with 40-Mflop computers, with results comparable in quality to the simultaneous analysis of all data. The reference frames for the global and network solutions can be free of distortion imposed by erroneous fiducial constraints on any sites.

Introduction

The Global Positioning System (GPS) has emerged in the 1990s as the space geodetic technique with the simultaneous virtues of accuracy and economy [e.g., *Yunck*, 1995]. It has been applied to a variety of geophysical phenomena, including the motion of tectonic plates [*Larson and Freymueller*, 1995; *Argus and Heflin*, 1995], plate-boundary deformation [*Feigl et al.*, 1993], motion associated with earthquakes [*Blewitt et al.*, 1993; *Bock et al.*, 1993], and changing Earth orientation [*Herring et al.*, 1991; *Lindqwister et al.*, 1992] and rotation rate. More recent uses of GPS include volcano monitoring [*Webb et al.*, 1995], ground-based measurements for atmospheric [*Businger et al.*, 1996] and ionospheric [e.g., *Wilson et al.*, 1995] applications, as well as atmosphere and ionosphere sounding [*Melbourne*, 1995] using low-Earth orbiters equipped with GPS receivers.

In heavily populated regions of significant seismic activity, deployment of dense networks of precision GPS receivers is in progress. Already hundreds of receivers are in operation in Japan and dozens in southern California. Networks such as these allow the on-going measurement of the surface deformation field and are expected to be valuable both in understanding the complex system of faults in the region and also in hazard mitigation. Additionally, space-based arrays of GPS-equipped receivers are expected over the next few years to exploit the potential applications of GPS to climate, weather, and the ionosphere.

Paper number 96JB03860.
0148-0227/97/96JB-03860$09.00

The volume of GPS data is growing rapidly, and a means to analyze this volume in a consistent, robust, and economical manner is essential. In this article we first discuss the computational burden associated with processing GPS data in the context of data volume and number of parameters estimated. We show that the computational burden associated with the rigorous least squares analysis of data simultaneously from R receivers scales with R^3. To the extent that global parameters, that is, orbits of GPS satellites (expressed in an Earth-fixed reference frame) and satellite clocks, can be estimated with a subset of the R receivers, then data from the others can be analyzed one at a time. Various analyses of data from $R = 49$ receivers are used to quantify the approximations involved in this technique, which we call "precise point positioning." The validity of the technique is also demonstrated based on data from over 10^2 receivers and 10^4 station days.

Computational Burden

The two GPS data types, carrier phase (L) and pseudorange (P), measure the receiver-to-transmitter distance with and without, respectively, an unknown bias. L is a much less noisy measurement than P, which offsets the fact that it requires estimation of a bias term. Both data types exist at each of two frequencies, approximately 1.2 and 1.6 GHz; this allows the formation of the ionosphere-free linear combination for each, which to first order is independent of the ionospheric electron density. We assume in what follows that we have formed this combination for L and P.

A phase measurement at time t between receiver r and transmitter x is modeled as

$$\begin{aligned} L_{rxt} &= \rho_{rxt} + b_{rxt} + z_{rt} m(\theta_{rxt}) \\ &\quad + \omega_{rxt} + C_{rt} - c_{xt} + \nu_{rxt}, \end{aligned} \tag{1}$$

where ρ_{rxt} is the true range, b_{rxt} is the phase bias or ambiguity, z_{rt} is the zenith tropospheric delay, $m(\theta_{rxt})$ is the mapping function for elevation angle θ_{rxt} between receiver and transmitter, and ω_{rxt} is the phase windup term to account for changes in the relative orientation of the receiving and transmitting antennas [*Wu et al.*, 1993]. Receiver and transmitter clock corrections are C_{rt} and c_{xt}, respectively. The term ν_{rxt} accounts for data noise in the measurement of phase to make (1) an equality. A pseudorange measurement is similarly modeled as

$$P_{rxt} = \rho_{rxt} + z_{rt}m(\theta_{rxt}) + C_{rt} - c_{xt} + \eta_{rxt}, \quad (2)$$

where η_{rxt} accounts for pseudorange data noise. Implicit in ρ_{rxt} are receiver coordinates and all nonclock transmitter parameters.

Undifferenced Data

Consider data from R receivers spanning a period Δ; typically we might have $\Delta = 24$ hours. Let δ be the time between measurements and let $\Omega/4\pi$ be the average probability that a satellite is in view above an assumed elevation cutoff (≈ 0.25 for a 15° cutoff). If there are X transmitters ($X = 24$ for the operational GPS constellation), then the number of measurements is given by

$$m = RX(\Omega/4\pi)(\Delta/\delta)d, \quad (3)$$

where d is the number of data types. Normally, $d = 2$, corresponding to ionosphere-free phase and pseudorange.

The number of parameters to be estimated can be written

$$n = aR + bX + c. \quad (4)$$

For example, station-specific parameters might include three Cartesian coordinates, a zenith tropospheric delay parameter, a clock parameter, and one phase bias parameter for each transmitter in view by the receiver over the period of interest. Thus $a = 5 + X$ in (4). Transmitter-specific parameters might include epoch-state position and velocity, two solar radiation parameters, a Y bias parameter, and a clock parameter, giving $b = 10$. In the case that transmitter parameters are fixed, we have $b = 0$. Polar motion values and rates are estimable with GPS, as is length of day, giving $c = 5$.

Over the period Δ it is essential to allow stochastic variation of clocks because most receiver and transmitter clocks look like white noise on timescales of minutes. Temporal variation of phase biases is also necessary to account for abrupt changes when the receiver loses lock or slips a cycle. Stochastic variation for zenith tropospheric delays and solar radiation parameters has also been found to be effective. Because we use square root information filter (SRIF) sequential estimation [*Bierman*, 1977; *Lichten*, 1990], such parameters contribute only once to the parameter count; the above expressions for a and b reflect this. SRIF sequential estimation is used because it is numerically stable and allows considerable flexibility for stochastic variation of parameters. It is approximately a factor of 2 slower than least squares estimation using normal equations.

The least squares estimate of n parameters with m measurements requires a number of arithmetic operations

$$B \propto n^2 m, \quad (5)$$

where the constant of proportionality depends on the choice of estimation algorithm but is of order unity [*Bierman*, 1977]. We neglect terms involving n^3 and nm because they are small compared to n^2m in this application. Thus (3), (4), and (5) give

$$B = kR^3 + \cdots, \quad (6)$$

where the ellipses denote terms of order R^2 and lower. The value of k is easily shown to equal $(5 + X)^2 m_1$, where m_1 is the number of measurements per receiver ((3) with $R = 1$). In (6) we assume that the constant of proportionality in (5) is 1.

Total processing times include three passes through the filter module. Identification of phase-bias breaks is performed after the first, and the third represents an iteration, required because of nonlinearities in our modeling of eclipsing satellites' yaw attitude [*Bar-Sever et al.*, 1996]. Total processing times also include auxiliary modules for input/output, data cleaning, calculations of predicted measured values and their derivatives with respect to estimated parameters, and so on. Shown in Figure 1 are actual processing times as a function of R, as well as the theoretical filter times using (5), with $X = 24$, $\Omega/4\pi = 0.25$, $\Delta = 30$ hours, $\delta = 5$ min, $d = 2$, $a = 29$, $b = 10$, and $c = 5$. From Figure 1 it is clear that somewhere in the region $50 \leq R \leq 100$, simultaneous analysis of data from R receivers starts to become computationally infeasible with 40-Mflop computing devices.

Partitioning

One method to reduce the burden is to divide the data into J groups. For simplicity we will assume that there are $J = 2$ groups with $m/2$ measurements in each. Let κ be the number of parameters common to both groups divided by the total number of parameters n. Then $(1 - \kappa)n/2$ parameters apply to the first group only, and another $(1 - \kappa)n/2$ apply to the second group only. In the context of the GPS problem each data partition could correspond to a distinct group of receivers; each receiver belongs to one and only one group. The common parameters are Earth orientation and satellite parameters, while the group-specific parameters are the parameters of receivers in the group.

The $m_1 = m/2$ measurements in group 1 are used to estimate $n_1 = \kappa n + (1 - \kappa)n/2 = (1 + \kappa)n/2$ parameters, requiring $n_1^2 m_1 = n^2 m(1 + \kappa)^2/8$ operations. The solution for the second group will require an equal number of operations, so that together the two solutions cost $n^2 m(1 + \kappa)^2/4$ operations.

Next, the two solutions must be combined. For the combination one can think of n parameters being determined from $n_1 + n_2$ measurements, costing

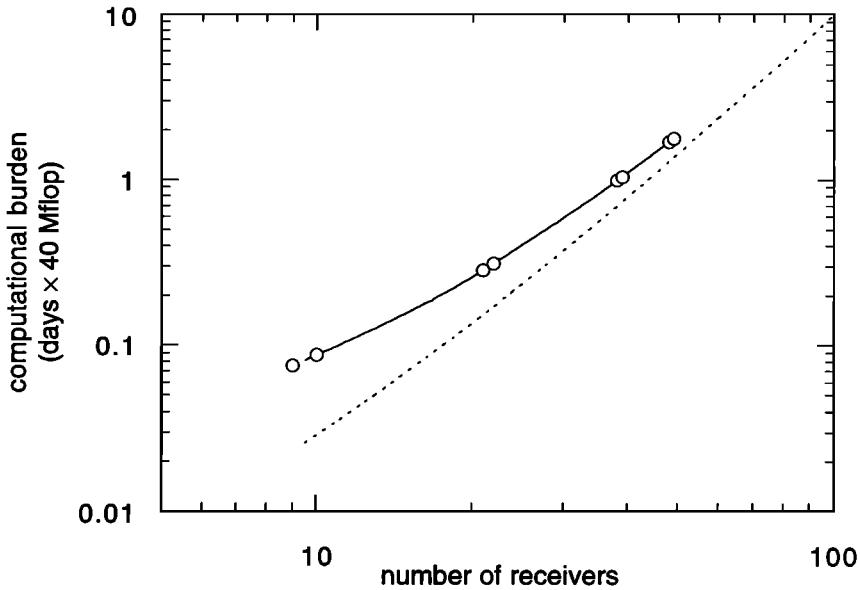

Figure 1. Computational burden B as a function of the number of receivers R. The open circles are actual total processing times on a 40-Mflop computer and include three passes through the parameter estimation module, as well as auxiliary programs. The dotted line is the theoretical time required for three passes through the parameter estimation module only, assuming $B = 2.68\, n^2 m$; the 2.68 is chosen so that Equations (3), (4), and (5) give the observed filter execution time for the $R = 48$ and 49 cases. The units of B are the number of days required by a 40-Mflop computer to perform the analysis.

$n^2(n_1 + n_2) = n^3(1 + \kappa)$ operations. The total cost χ, relative to the $n^2 m$ operations required for the analysis of all data simultaneously, is thus

$$\chi = (1 + \kappa)\left[\frac{1 + \kappa}{4} + \frac{n}{m}\right].$$

This can be generalized to

$$\chi = [1 + \kappa(J - 1)]\left[\frac{1 + \kappa(J - 1)}{J^2} + \frac{n}{m}\right] \qquad (7)$$

when the m measurements are divided equally into J groups. Note that (7) approaches unity as $\kappa \to 1$, assuming n/m is small. Thus, if all parameters are common, partitioning is ineffective.

With $X = 24$, $\Omega/4\pi = 0.25$, $\Delta = 24$ hours, $\delta = 5$ min, $d = 2$, $a = 29$, $b = 10$, $c = 5$, and $R = 40$ receivers, we have $n = 1405$ parameters of which

$$\kappa n = bX + c = 245$$

are common ($\kappa \approx 0.174$). There are $m = 138240$ measurements, and the ratio of parameters to measurements is $n/m \approx 0.01$. Equation (7) then shows a 64% reduction in burden for $J = 2$ and an 88% reduction for $J = 40$. Clearly, partitioning is one effective means of reducing CPU when κ is small and has been demonstrated by some analysis centers in the International GPS Service for Geodynamics (IGS).

When many parameters are treated as stochastic, rigorous partitioning is difficult. We feel that the benefits of using stochastics outweigh this disadvantage.

Double Differencing

For receivers q and r in view of satellites w and x at time t, (1) can be used to show that the quantity

$$dL_{qrwxt} \equiv L_{qwt} - L_{rwt} - L_{qxt} + L_{rxt} \qquad (8)$$

is independent of all clock parameters. In practice, synchronization of all measurements to GPS time is made prior to the formation of the double difference. A similar double difference can be formed for the pseudorange. Least squares estimation of nonclock parameters can be made based on double-difference measurements. It is straightforward to form a measurement covariance matrix that accounts for known correlations in double-differenced data.

The technique has the advantage of a reduction in both the measurement and parameter counts. One need not include the entire set of double-difference measurements because it contains redundant information. For R receivers in view of X transmitters at time t there are $(R - 1)(X - 1)$ independent double differences that form a complete measurement set. One such set is dL_{qrwxt} for $q = w = 1$, $2 \le r \le R$, and $2 \le x \le X$. Thus the measurement count m is reduced by $RX - (R-1)(X-1) = R + X - 1$ compared to the undifferenced case. An identical reduction in the parameter count n occurs because $(R - 1)(X - 1)$ is also the number of phase bias parameters to be estimated, compared with RX in the undifferenced case. Finally, receiver and transmitter clocks are no longer parameters, so that the parameter count is further reduced by $R + X$.

For $X = 24$, then, the value of n^2m is reduced by about 34% for $R = 10$ and by 19% for $R = 100$. From the standpoint of computational burden the double-difference approach has approximately this advantage over the undifferenced approach when data from R receivers are simultaneously analyzed.

To simplify the calculation, we have ignored the extra computational burden needed to form the double differences and a measurement covariance matrix that accounts for known correlations in data noise. We have also ignored issues of common visibility by assuming that all R receivers view all X transmitters at all times. Although *Blewitt* [1993] gives an example of a case in which it is not possible to form a set of double differences which contains all of the information content available for estimation of nonclock parameters, performance of IGS analysis centers that use double differencing indicates that this is not a practical limitation.

The double-difference technique views receiver and transmitter clocks as nuisance parameters that can be eliminated up front by the appropriate linear combination of data [*Wu*, 1984], exactly analogous to eliminating ionospheric effects by forming the ionosphere-free combinations described earlier. In the method described here, however, transmitter clock parameters, together with GPS orbits, are the key for the efficient analysis of large networks of GPS receivers. (From the point of view of information content as opposed to computational burden, consult *Kuang et al.* [1997] for comparisons of the differenced and undifferenced approaches.)

Precise Point Positioning

Suppose data from a globally distributed network of R receivers are used to estimate receiver and transmitter parameters. Denote the estimates of transmitter parameters by $\mathbf{P}$. Consider an additional receiver and the analysis of data from $R+1$ receivers to yield transmitter parameters $\mathbf{Q}$. In the approximation that $\mathbf{P} = \mathbf{Q}$, that is, data from the additional receiver has negligible effect on the values of estimated transmitter parameters, a more efficient way to estimate the parameters specific to the additional receiver is to analyze data from it in seclusion and fix the transmitter parameters in the analysis to be $\mathbf{P}$. When GPS orbits in an Earth-fixed frame and GPS clock corrections are not estimated but, instead, fixed at some predetermined values and the model has no other spatially correlated parameters (e.g., tropospheric delay), then there is no need to analyze data from all receivers simultaneously.

The term "point positioning" in GPS analysis has referred historically to the estimation of receiver-specific parameters by the analysis of receiver pseudorange data, fixing transmitter parameters to values broadcast in the navigation message. The quality of results is limited in this case because (1) pseudorange is inherently noisy, no better than about 40 cm, based on our experience with postfit residuals of geodetic-quality GPS receivers and (2) the transmitter parameters broadcast in the navigation message are accurate to a few meters for GPS orbits or a few tens of meters for GPS clocks [*Zumberge and Bertiger*, 1996]. Our use of precise point positioning differs from the classical use of the term in two ways. First, both carrier phase and pseudorange are used as data. Second, the quality of transmitter parameters is a few centimeters or better. When applied to single-receiver data, the resulting accuracies are comparable to what is obtained when data from all receivers are simultaneously reduced and come at far lower computational cost.

Method

Suppose the analysis of data from R receivers is divided into two parts. First, a subset of S receivers is used to estimate satellite parameters, Earth orientation, and S sets of receiver parameters. Then, data from each of the remaining $R - S$ receivers are analyzed, one receiver at a time. The computational burden B can be written as the sum of two terms, one for the global solution (B_g) and one for the point-positioned sites. For the global solution we have $n_g = aS + bX + c$ parameters to estimate from $m_g = SX(\Omega/4\pi)(\Delta/\delta)d$ measurements. The corresponding burden is $B_g = kS^3 + \cdots$, just as in (6) with R replaced by S.

The computational burden to determine $n_1 = 5 + X$ receiver-specific parameters given m_1 ((3) with $R = 1$) measurements is $B_1 = n_1^2 m_1$; this applies to $R - S$ sites. The total burden is thus $B = B_g + (R - S)B_1$ or

$$B = (5 + X)^2 m_1 (S^3 + R - S) + \cdots. \quad (9)$$

The S^3 term totally dominates, so that the receiver parameters from the additional $R - S$ sites are essentially free. Note that the computational burden includes the parameter-estimation processes only. The total point-position computational burden is of the order of 1 min per site on a 40-Mflop computer.

Aside from computational efficiency an additional advantage of the one-receiver-at-a-time processing is that it allows easy diagnosis of receiver-specific problems. For geodetic quality receivers the rms value of the postfit residuals, that is, the rms difference between the modeled values in (1) or (2) and the measured values, is 5 to 10 mm for phase and 50 to 100 cm for pseudorange. If measurements from a particular receiver are significantly noisier, it may be an indication of a hardware fault, a poor multipath environment, an interfering RF source, or other unusual circumstance.

Reference Frame

One way to impose a reference frame in the analysis of GPS data is to assume that coordinates of certain sites are sufficiently well known that they can be fixed or tightly (< 1 cm) constrained in the analysis of data from a global network [*Blewitt*, 1993, and references therein]. For example, the analysis centers of the IGS fix the locations of 13 globally distributed sites in their determinations of precise GPS ephemerides [*Kouba*, 1995].

A disadvantage to the fiducial approach is that errors in assumed locations of the fiducial sites distort the

GPS orbits in a way that is not easily undone. (This disadvantage does not apply to site coordinates produced by IGS analysis centers; such coordinates do not reflect strong fiducial constraints.) In our experience at JPL's (Jet Propulsion Laboratory) IGS analysis center [*Zumberge et al.*, 1995], such "errors" can arise in two ways. First, the "standard" reference frame, the International Terrestrial Reference Frame (ITRF) [*Boucher et al.*, 1994] in the case of the IGS, itself evolves with time, so that a discontinuity in assumed locations of fiducial sites will occur, typically at midnight between two calendar years. These discontinuities are not related to actual motion of sites but indicate only a change in assumed locations.

Fiducial orbits on December 31, 1994, that are based on ITRF 92, for example, will exhibit a discontinuity compared with orbits on January 1, 1995, that are based on ITRF 93. These discontinuities are small, typically a few centimeters and can be reduced by applying a seven-parameter Helmert transformation but only to the extent that the two reference frames are related by such a transformation. Without reprocessing the discontinuities cannot be entirely eliminated, and a time series of results derived from fixed-orbit analyses will inherit the discontinuities. The effect can be several millimeters in positions.

Second, mistakes in assumed antenna heights of fiducial sites, or other similar blunders, cannot be completely eliminated. Expensive reprocessing of global data will be required if the mistakes are significant enough.

To avoid the consequences of fiducial errors, a priori uncertainties of coordinates are set fairly large at 1 km (10 m for the site at Algonquin Park, Canada). Although the resulting "free-network" solution will be in a poorly defined reference frame, all estimated parameters will be immune to fiducial errors, and expensive reprocessing of global network data is avoided. Furthermore, a particular reference frame can be realized by transforming estimated receiver parameters into that frame. A different frame (an updated ITRF, for example) can be realized simply by applying a new transformation. Estimated parameters of sites subject to precise point positioning with free-network transmitter parameters will be in the same reference frame as the original free-network solution. A single seven-parameter transformation can be applied to all sites for alignment with the ITRF. The appropriate transformation should be available to users from the analysis center that produced the free-network orbits and clocks. The free-network approach has been demonstrated for Earth orientation [e.g., *Herring et al.*, 1991], baselines [*Heflin et al.*, 1992], coordinates [*Blewitt et al.*, 1992], and velocities [*Feigl et al.*, 1993; *Argus and Heflin*, 1995].

Single-Day Tests

Transmitter parameters. Shown in Figure 2 are sites from which various networks are constructed to

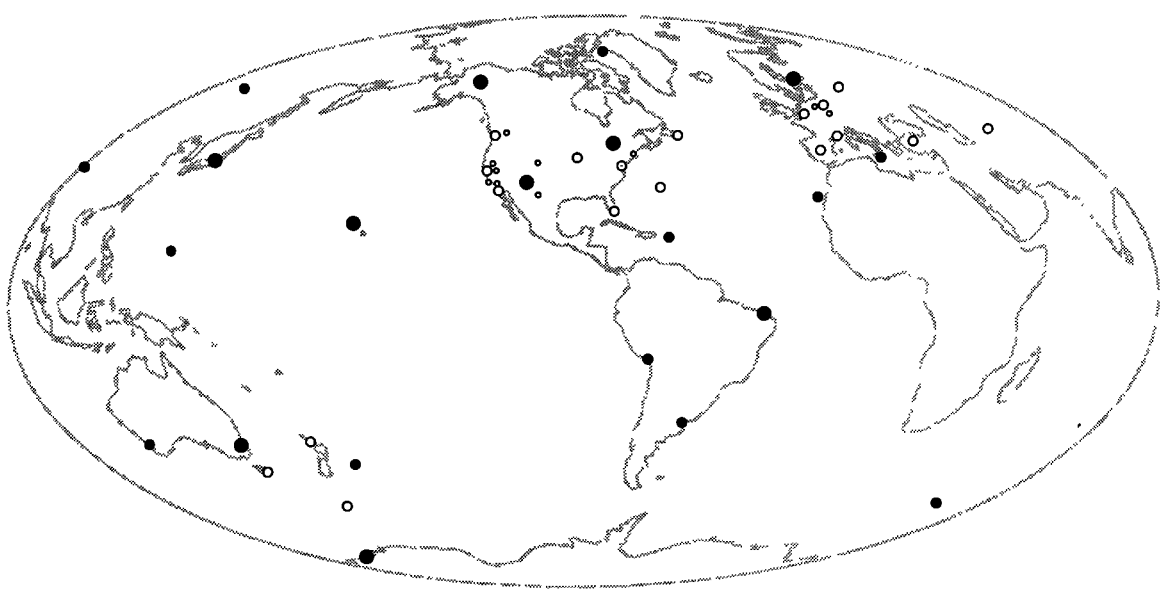

Figure 2. Sites used for tests of point positioning. The nine large solid circles correspond to receivers at, from left to right, Usuda, Japan; Tidbinbilla, Australia; Kokee Park, Hawaii; Casey, Antarctica; Fairbanks, Alaska; Pietown, New Mexico; Algonquin Park, Canada; Fortaleza, Brazil; and Metsahovi, Finland. The 12 smaller solid circles correspond to receivers at Lhasa, China; Perth, Australia; Guam, Pacific Ocean; Irkutsk, Russia; Chatham Island, New Zealand; Thule, Greenland; Arequipa, Peru; St. Croix, U.S. Virgin Islands; La Plata, Argentina; Maspalomas, Canary Islands; Noto, Italy; and Kerguelen Islands, Indian Ocean. The dotted open circles correspond to three sites in Australia and New Zealand, eight sites in North America, and seven sites in Eurasia. Finally, the small open circles correspond to additional sites in North America (eight) and Europe (two). Although there are permanently operating receivers in the southern Pacific Ocean and Africa, their data on November 1 were either not available or of poor quality.

Table 1. Average Formal Errors of Transmitter Parameters Estimated From Different Networks of Figure 2

S	Orbit 3-D, cm	Var, cm	Coverage, %	Clock, cm	Var, cm
9	19.4	5.9	90.5	9.7	3.5
10	16.7	4.4	90.9	8.9	3.1
21	6.1	1.0	98.9	4.7	0.4
22	5.9	1.0	98.9	4.6	0.4
38	4.6	0.7	98.9	3.8	0.3
39	4.6	0.7	98.9	3.8	0.3
48	4.4	0.7	98.9	3.7	0.3
49	4.4	0.7	98.9	3.7	0.3

The nine-station network is shown as the nine large solid circles in Figure 2. The 21-station network includes, in addition, the 12 smaller solid circles. The 39-station network includes the 21 plus an additional 18 indicated by the dotted open circles. Finally, the 49-station network includes all sites in Figure 2. Networks with $S = 10, 22, 38, 48$ consist of the network with $S \pm 1$ receivers, with the addition or subtraction of the receiver in Belgium (a dotted open circle in Figure 2). Thirty hours of data centered on GPS noon, November 1, 1995, were analyzed. The coverage column indicates that for the 9- and 10-station networks the geometry was insufficient to determine clock parameters about 9% of the time. The var columns indicate the 1-standard-deviation variability in the formal errors among satellites and over time for the 24-hour period of November 1, 1995. To remove contributions from reference-frame uncertainties, the locations of the nine large solid circles in Figure 2 are assumed known for purposes of Table 1 only.

determine transmitter parameters, in the Earth-fixed frame, based on November 1, 1995, data. The solid circles compose a network of 21 stations with good global distribution. This network consists of a sparse nine-station network (large solid circles) with reasonable global coverage except near 90°E longitude and an additional 12 sites (small solid circles) chosen to give improved global distribution.

Given the distribution of receivers shown in Figure 2, the uniformity of the global distribution cannot be improved much beyond this 21-station network. Shown in Table 1 are the formal errors of estimated transmitter parameters as a function of the network used as data, assuming that the locations of the nine large solid circles in Figure 2 are precisely known. This assumption is similar to one made by IGS analysis centers in producing fiducial orbits. In the present article it is invoked only so that the formal errors of the transmitter parameters will not reflect reference-frame uncertainties. Free-network estimated transmitter parameters are used in all analyses.

Table 1 shows that $S = 9$ provides estimates of orbits and clocks that are, on the average, determined with formal errors that are factors of 4.4 and 2.6, respectively, larger than those determined with $S \geq 38$. Furthermore, the $S = 9$ and $S = 10$ networks have large variations in the formal errors, as well as geometry that is insufficient to determine clock parameters for about 10% of the time and/or satellites.

On the other hand, Table 1 also indicates that for $S \geq 21$ the reduction in formal error that accompanies the increase in S is somewhat less than would be expected from $1/\sqrt{S}$, because (1) the contribution due to reference-frame uncertainty has been removed, as discussed above, and (2) the additional sites are clustered in already populated regions.

To what extent do the data from additional receivers affect the estimated transmitter parameters? Shown in Figure 3 is a comparison of transmitter parameters

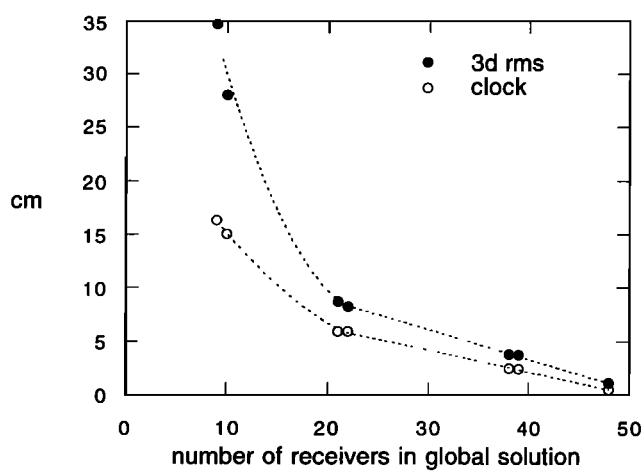

Figure 3. Transmitter parameters determined with fewer than 49 receivers, compared with those determined from the 49-station solution. The solid circles give the three-dimensional rms difference in satellite positions, while the open circles give the rms difference in clock solutions. The gradual improvement beyond 20 receivers in the global solution is costly in terms of computational burden.

Table 2. Formal Errors in Coordinates of Point-Positioned Sites

	North, mm	East, mm	Vertical, mm	3-D, mm
Average	0.8	2.0	4.8	5.2
Variation	0.2	0.5	0.7	0.8

These reflect only assumed data noise (1 m for P and 1 cm for L), the sampling interval, and a priori uncertainties in estimated receiver parameters. The data noise contribution dominates. By definition of point positioning, orbit and clock errors do not contribute to the formal errors. Thus formal errors are essentially independent of the network from which global parameters were derived. (However, because of incomplete coverage as indicated in Table 1, formal errors of point-positioned sites based on orbits and clocks derived from the 9- and 10-station networks are slightly, about 8%, larger than for the other networks.) The average row indicates the average value over all sites in Figure 2, and the variation row indicates 1-standard-deviation variability.

estimated from different subsets of the sites shown in Figure 2. To avoid contributions to the uncertainties that arise from imperfect knowledge of receiver coordinates only weak, 10-m to 1-km, a priori constraints are imposed on these, as described earlier. Because the resulting transmitter parameters are in a poorly defined Earth-fixed reference frame, the rms differences shown are after a seven-parameter (three translations, three rotations, and a scale factor) transformation to align, orient, and scale the reference frames to each other.

From Figure 3 it can be seen that the 9- and 10-station networks provide transmitter parameters that differ by tens of centimeters from those estimated with $S \geq 21$. On the other hand, the differences among the $S \geq 21$ networks is of the same order as the formal errors. Such differences may not be worth the significant increase in computational burden from $S = 21$ to $S = 49$.

Receiver parameters. Another measure of the technique's validity is the degree to which estimated receiver parameters depend on the division of the total $R = 49$ sites into S used in the global solution and the $R - S$ sites that are subsequently point positioned. For reference we show in Table 2 the formal errors of point-positioned sites. By definition, uncertainties in estimated transmitter parameters do not contribute to formal errors in point-positioned sites and so are essentially independent of S. (The exception has to do with $S = 9$ and 10, for which insufficient coverage means that transmitter clocks were not estimable about 10% of the time.) The formal errors are about 1 mm in the north component, 2 mm in the east, and 5 mm in the vertical.

To improve estimates of transmitter parameters near the midnight boundaries, the global solution uses 30 hours of data centered on GPS noon of November 1, 1995. Receiver parameters determined in the global solution correspond to the same 30 hours, whereas point-positioned solutions correspond to only 24 hours of receiver data. To force all receiver parameters to correspond to the same interval, point positioning is applied to 24 hours of data from each of the 49 sites, and all receiver parameters are reestimated. For the $S = 49$ solution, the rms differences in receiver coordinates due to this change in Δ are 0.7 mm in the north, 2.6 mm in the east, and 5.4 mm in the vertical.

Shown in Figure 4 are the differences in estimated receiver parameters as a function of S, with $S = 49$ as the basis for comparison. To account for the reference frame uncertainty of the free-network transmitter parameters, all solutions are aligned to the 39-station results, using a seven-parameter Helmert transformation to minimize the rms coordinate difference of the nine-station network. Clearly, the $S = 9$ and $S = 10$ networks give rise to several tens of millimeters differences in estimated receiver parameters. Beginning with $S = 21$, however, receiver parameters are less and less affected, and differences are comparable to the formal errors.

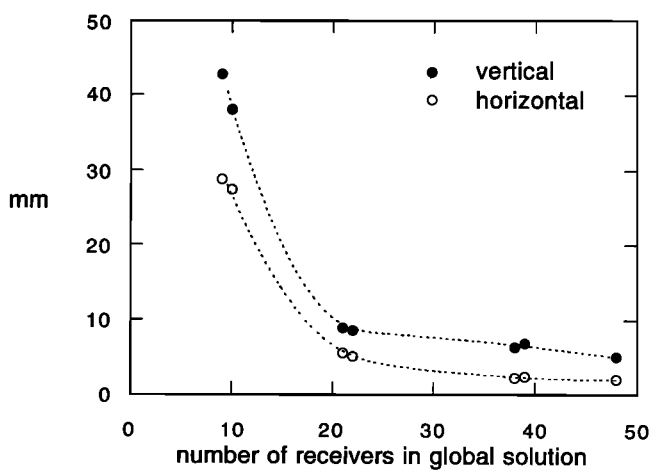

Figure 4. Point positioning rms differences over all sites in Figure 2, showing the effect of different divisions of $R = 49$ sites into S used to determine transmitter parameters. All solutions are aligned to the 39-station results, using a seven-parameter Helmert transformation to minimize the rms coordinate difference of the nine-station network. Above 20 receivers in the global solution, receiver parameters do not depend very strongly on the division. The horizontal points refer to the sum in quadrature of the north and east components.

We have also computed the rms coordinate differences for the 11 stations that participated in the $S = 49$ global solution but not that for $S = 38$. That is, if one uses the $S = 38$ network to determine transmitter parameters, then uses those and precise point positioning for 11 additional stations, how do the results compare with the inclusion of the 11 stations in the global solution? The answer is 2.5-mm rms in the horizontal and 9.1-mm rms in the vertical. (If the site with the largest vertical difference is excluded, the rms vertical is reduced to 6.8 mm.) For the vertical this value is slightly higher than that shown in Figure 4 for $S = 38$. On the scale of the formal coordinate errors of the 11 sites, 2.6 mm horizontal and 4.5 mm vertical, the differences are marginally significant.

(Since the $S = 48$ and $S = 49$ transmitter parameters differ by only about 1 cm or less (Figure 3), the 5-mm rms difference for the vertical component for the $S = 48$ solid circle in Figure 4 may seem somewhat high. However, this is most likely explained by the reestimation of receiver parameters once transmitter parameters are determined, so that all receiver solutions correspond to 24 hours instead of 30 hours, as described above.)

Geographical distribution and truth case. To evaluate the uniformity of S sites distributed on a sphere, we first define the function

$$R(\theta, \phi) \equiv \min [r_1, r_2, \cdots r_S],$$

where θ is colatitude, ϕ is longitude, and r_n is the great circle distance between (θ, ϕ) and site n. Thus $R(\theta, \phi)$ is the distance from (θ, ϕ) to the nearest of the S sites. The rms isolation is then

$$\zeta \equiv \sqrt{\frac{\int_0^{2\pi} d\phi \int_0^{\pi} d\theta \, \sin\theta \, R^2(\theta, \phi)}{4\pi}}. \qquad (10)$$

Shown in Figure 5 is a plot of ζ versus S, using Simpson's rule in two dimensions to numerically evaluate (10). Clearly, ζ decreases negligibly above $S \approx 21$, which is simply a consequence of large regions, oceanic areas and Africa, with no receivers. That is, in Figure 2 the distances from open circles, both dotted and small, to nearby solid circles are small compared to the distances from isolated regions to solid circles.

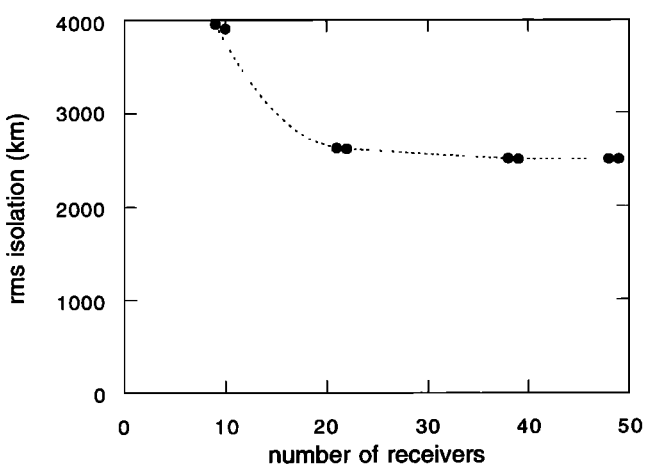

Figure 5. The rms isolation ζ (Equation 10) as a function of the number of receivers.

Figures 3 and 4 implicitly assume that the $S = 49$ solution is the "truth" case to which $S < 49$ results should be compared. From Figure 3 one might conclude that there is a slight but steady improvement in the quality of transmitter parameters for $S \geq 21$. To a lesser degree a similar conclusion might be drawn from Figure 4 in the case of receiver parameters. For several reasons, including mismodeling, it is not necessarily the case that $S = 49$ represents truth more than, say, $S = 38$.

Even with no mismodeling, Table 1 indicates only marginal improvement in the ability to determine transmitter parameters with increasing S beyond $S = 21$, given the distribution of sites as shown in Figure 2. In fact, for the site distributions and values of S used here, formal errors of transmitter parameters are approximately linearly related to ζ, with $d\sigma_1/d\zeta \approx 9.4$ cm per 10^3 km and $d\sigma_2/d\zeta \approx 3.8$ cm per 10^3 km, where σ_1 denotes the three-dimensional rms orbit formal error and σ_2 denotes the clock formal error. Thus an increase in S which is not accompanied by a decrease in ζ is of little value in improving the overall, global quality of transmitter parameters, even in the absence of mismodeling.

Furthermore, known aspects of mismodeling include a number of simplifying assumptions related to tropospheric delay, ocean loading, satellite force models, and variations in receiver and transmitter phase centers, to name a few. Because of the geographical distribution of receivers, the $S = 49$ solution will suppress manifestations of mismodeling, or systematic errors, more in Europe and North America than in other regions. In the presence of systematic errors the least squares solution for $S = 49$ may not be nearer to truth than that for $S = 21$ or $S = 38$. In addition to mismodeling, uneven data quality from common or additional stations could cause the $S = 49$ solution to be better or poorer, respectively, than that for $S = 38$.

Weekly reports by the IGS analysis coordinator (see http://igscb.jpl.nasa.gov/IGSREPORT.html) evaluate the quality of estimated transmitter parameters from all IGS analysis centers. The number of receivers used varies with center and ranges from fewer than 30 to over 100. There is almost no correlation, however, between the quality of transmitter parameters and the number of sites. Our interpretation is that beyond $S \approx 30$ with the global distribution as in Figure 2, the value of data from additional receivers in determining transmitter parameters is marginal at best and may even be outweighed by systematic errors. As new receivers are installed in currently isolated regions thereby moving the ζ curve downward, we of course expect that data from these new receivers will be valuable in determining transmitter parameters. As of November 1996, the global distribution is such that analysis of data from approximately 35–40 well-distributed sites is appropriate.

Multi-Day Tests

The operational GPS analysis at JPL [*Zumberge et al.*, 1995] has been in place since 1992. Shown in Figure 6 is the detrended time series of coordinates for the receiver at JPL spanning 2.5 years following the Northridge earthquake of January 17, 1994. The 109 circles correspond to days when data from this receiver were included in the global solution, while the 426 shaded points correspond to coordinates determined from precise point positioning. The distributions of the daily deviations are also shown. From Figure 6 it is clear that there is little or no discernible difference between the two classes.

Point position time series from 151 sites can be viewed at http://sideshow.jpl.nasa.gov/mbh/series.html. Histograms of daily repeatabilities based on these are shown in the left of Figure 7. Repeatability is about the estimated linear trend. Sites with known and uncorrected changes in antenna height are not included, leaving 139 sites. The number of days for a given site ranges from a few to a few hundred; the median value is 106 days.

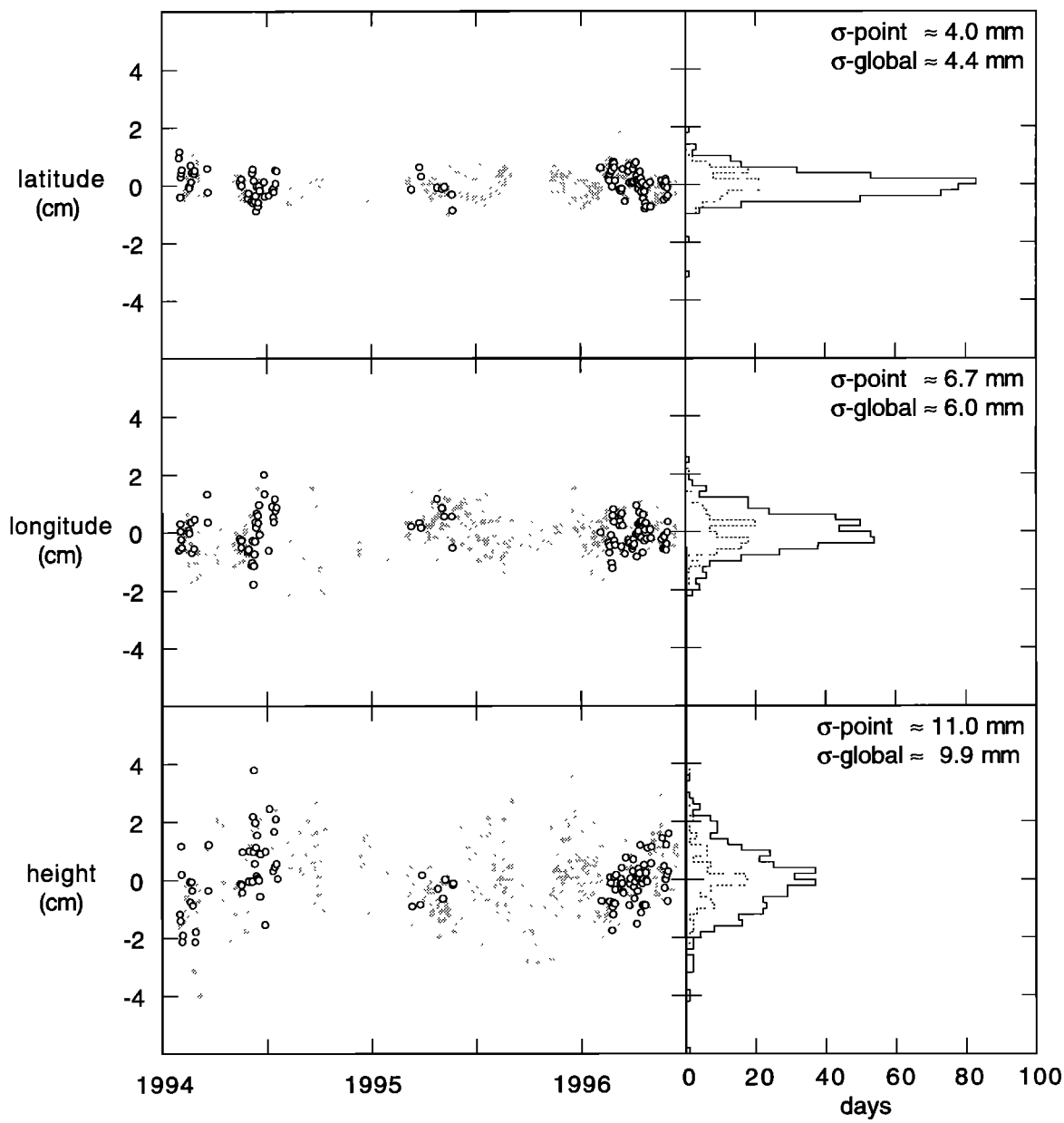

Figure 6. Time series of geocentric coordinates (detrended) for the receiver at the Jet Propulsion Laboratory (JPL), beginning late January 1994 after the Northridge earthquake. The open circles indicate 109 days when JPL data were included in the daily global solution. The shaded points indicate 426 days when JPL data were analyzed with precise point positioning. Shown also are the distributions of deviations for the global (dotted line) and point-positioned (solid line) solutions; the histograms have a 2-mm bin width. The differences in the means and widths (σs) of the distributions are both small and statistically insignificant.

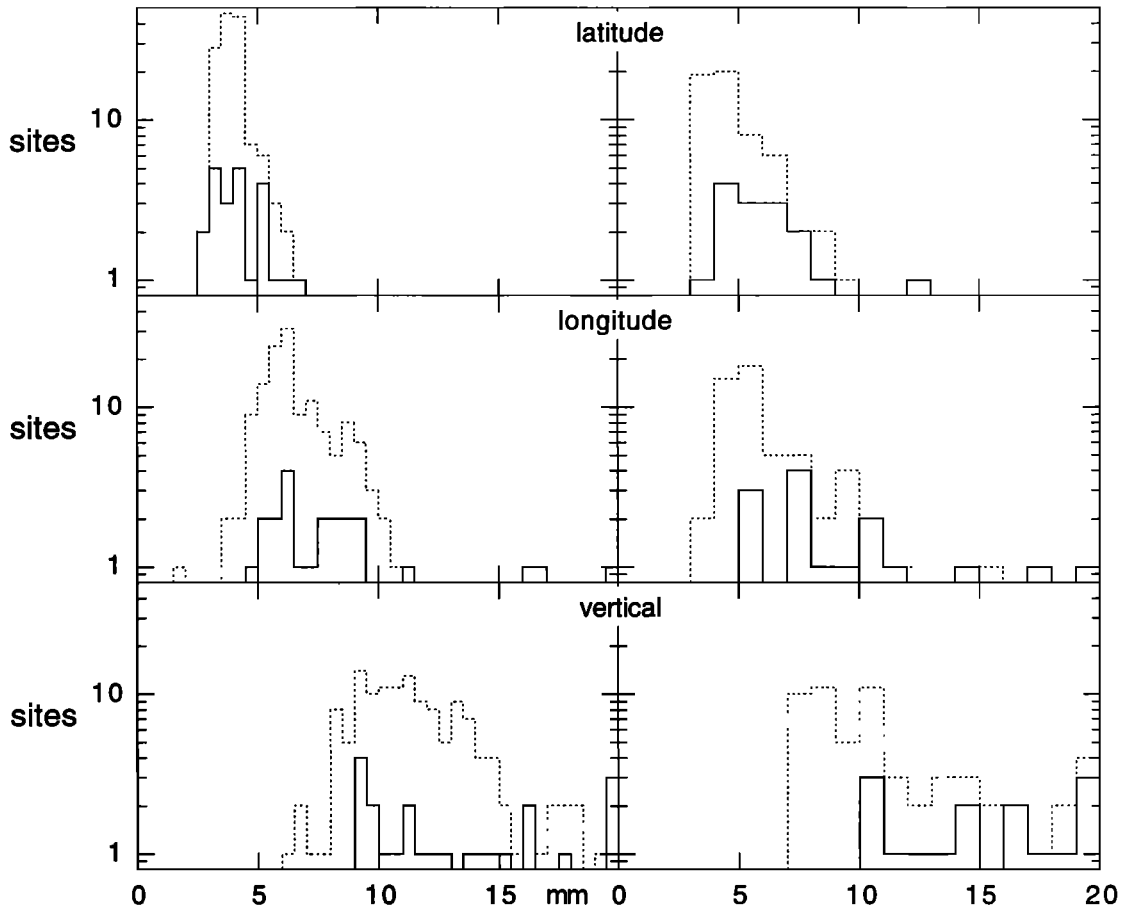

Figure 7. Distributions of daily repeatabilities (dotted lines) for 139 sites (left) that have been analyzed with precise point positioning and 59 sites (right) that participated in many daily global solutions. The solid lines indicate sites in the southern hemisphere (23 on the left and 15 on the right). The median values are 3.9 mm in latitude (north), 6.3 mm in longitude (east), and 11.1 mm in the vertical for the point-positioned sites and 4.4 mm in latitude, 5.6 mm in longitude, and 10.3 mm in vertical for global sites.

Except for a few outliers, some of which are due to receivers with a history of poor performance, the repeatabilities do not vary too much from site to site and, in particular, do not depend strongly on northern versus southern hemisphere. The median values are 3.9 mm for the north component, 6.3 mm for the east, and 11.1 mm for the vertical.

For comparison, the corresponding values for 59 sites included in global analyses are 4.4 mm, 5.6 mm, and 10.3 mm; their distributions are indicated on the right of Figure 7. The differences are insignificant. What was demonstrated in detail for the site at JPL (Figure 6) is thus true in general.

Mismodeling

There are several high-precision software systems currently in use to analyze GPS data, of which Gipsy-Oasis II (GOA-II) used in this work is one. Can satellite parameters determined with one system be used in another? To the extent that there is consistency among software systems in how GPS observables are modeled as a function of these parameters, the answer is yes.

It is well known that details of an estimation strategy (the choice of relative weight between pseudorange and phase measurements, the a priori uncertainties in parameters, and the model of troposphere temporal variability) can change the estimated values of parameters with little change in the quality of the fit, reflecting some degree of degeneracy among parameters. Nevertheless, the concept of satellite clock is no less valid in principle than that of satellite orbit. For GOA-II the formal errors of orbits and clocks from Table 1 indicate that to the few-centimeter level or better there is strength in the data to determine them separately from other parameters.

Comparisons among results from seven different IGS analysis centers using six distinct software systems have shown that estimated parameters from different analyses agree to (1) about 20 cm, three-dimensional (3-D) rms, for daily orbits; (2) a few millimeters for horizontal station coordinates, averaged over 7 days; (3) about 1 cm for vertical station coordinates, averaged over 7 days; and (4) about 5 mm for daily estimates of total zenith tropospheric delay. These levels of agreement in-

dicate that the modeling among the different systems is very similar.

To further quantify the level of mismodeling, or different modeling, among the different systems, we have applied precise point positioning to 94 sites, globally distributed, using data from March 4, 1996. GOA-II was used for all analyses, but there were two different sets of satellite parameters used: (1) JPL clocks determined every 5 min and JPL orbits and (2) GeoForschungsZentrum (GFZ) [*Gendt et al.*, 1995] clocks determined every 30 min and GFZ orbits. Parameters from set 2 were retrieved from the NASA Crustal Dynamics Data Information Center (CDDIS) [*Noll*, 1995].

The 3-D rms variation in satellite positions over the day (March 4, 1996) between JPL and GFZ is 33 cm. (For the present purpose, fiducial orbits are used. The improvement in orbit agreements is negligible if a seven-parameter transformation is allowed, indicating good reference frame agreement between JPL and GFZ.) The rms agreement between JPL clocks and GFZ clocks is 23 cm. Because precise GFZ clocks are available from the CDDIS only at 30-min intervals, the data rate available for analysis is 6 times less frequent than for the JPL solutions (see discussion on selective availability in the section on limitations).

The rms differences in estimated site coordinates determined in set 2 relative to set 1 are reasonably good: 9 mm in the north, 16 mm in the east, and 28 mm in the vertical. (We have had less success in mixing orbits from one analysis center with clocks from another, possibly because of correlations in orbit and clock errors.) The dominant contributor to these values may be the decreased amount of data analyzed using GFZ transmitter parameters. To the question posed at the beginning of this section, we can thus say, yes, at the centimeter level. To establish this at the few-millimeter level awaits further work.

Limitations

One limitation to the precise point positioning technique is that the covariance matrix of estimated receiver parameters will not necessarily be indicative of the actual quality of results because (1) it will show no correlation between sites and (2) its nonzero elements will be independent of receiver location. Consequently, the covariance matrix may be inappropriate for some applications.

Because of point 1, if the location of one site from point positioning is estimated as $\vec{x}_a$ with covariance V_a and the location of another site is estimated as $\vec{x}_b$ with covariance V_b, then the baseline estimate between these sites is $\vec{x}_a - \vec{x}_b$ with covariance $V_a + V_b$. Common error sources, from transmitter parameters, for example, do not contribute to the individual covariances and cannot get removed in the formation of the vector difference.

Real measures of performance, like daily repeatability, will show an improvement if common error sources are differenced away. For example, repeatabilities of baselines formed from point-positioned results of southern California sites are smaller by 20%–60% compared to the single-site coordinate repeatabilities, depending on component, for baseline lengths up to about 200 km. That this is not reflected in the formal errors for baselines is the result of a compromise between mathematical correctness and computational feasibility.

(By examining the covariance matrix of estimated site coordinates among sites determined in our regular global solutions, we may be able to determine approximately correct site-to-site correlations for sites subject to precise point positioning. For example, $\rho_{ij} = e^{-\lambda d_{ij}}$ might model the correlation between sites i and j separated by distance d_{ij}, with λ an empirical parameter.)

A consequence of point 2 is that formal errors of point-positioned results from isolated sites will be no different from those in dense areas. We use "isolated" here in the sense that data from no nearby receivers were used in the global solution that produced the transmitter parameters. Transmitter parameters are probably not as well determined in such areas. This effect, already small as evidenced by the lack of strong northern/southern hemisphere dependence in Figure 7 (left), will become negligible as the global network continues its expansion.

A second limitation has to do with the availability of precise transmitter clock estimates. The technique will yield results of the quality shown here only when these are accurate to the few-centimeter (100 ps) level at each data epoch. Because of selective availability, GPS clocks vary by the order of 10^3 cm (10^1 to 10^2 ns) over timescales of minutes. Thus precise knowledge of their values every, say, 5 min is of no use in predicting their values more frequently, at least not to the few-centimeter level. As mentioned earlier, navigation-message clock corrections, though available in real time, are essentially linear approximations over $\approx 10^2$ min and are accurate only to the 10^3-cm level. Some participants in the IGS [*Kouba*, 1995] now routinely produce GPS clock estimates with subnanosecond precision at least as frequently as every 15 min and every 5 min from some centers. However, until precise GPS clocks are produced more frequently than once every minute and preferably once every 10 s, data to be analyzed with precise point positioning will have to be decimated to coincide with epochs for which precise GPS clock solutions exist.

To achieve subcentimeter results requires dual frequency, geodetic-quality receivers so that ionospheric variations can be differenced away and data cleaning can be done on a single-receiver basis. Whenever the results from a given receiver are limited by the accuracy of orbits and clocks in the broadcast message, however, use of precise clocks and orbits will provide an improvement, even for inexpensive receivers.

A detailed discussion of the integer resolution of phase bias parameters [*Blewitt*, 1989] is beyond the scope of this article. Because of receiver- and transmitter-specific phase delays, which are generally not known and may vary with time, it is only the double-difference phase biases that will be integers. Thus resolution of these parameters cannot be performed on point-positioned results from a single receiver. Results from

multiple point-positioned sites in a local network can be combined to resolve double difference phase ambiguity parameters, with reduction in baseline daily repeatabilities, especially for the east and vertical components.

For those applications that do not require accuracies better than a few millimeters in the horizontal dimension and approximately 1 cm in the vertical dimension, ambiguity resolution is not necessary, provided that the observation time is of the order of 1 day; for shorter observing times, ambiguity resolution is increasingly valuable. For applications involving long baselines, for example, global networks, ambiguity resolution is difficult at best. For dense regional networks the rigorous solution of resolving double-difference phase biases involving hundreds of sites is not computationally feasible. Most approaches use clusters of stations with overlapping subnetworks; these probably suffer some degradation when compared to a rigorous solution. Additional work is necessary to quantify the trade-off between computational feasibilty and mathematical rigor as it relates to ambiguity resolution.

Conclusions

We have shown that a robust and economical means of analyzing data from hundreds or more GPS receivers involves (1) analyzing a globally distributed subset to determine transmitter parameters (and receiver parameters for the subset) and (2) analyzing the remaining data one receiver at a time. The quality of results for station parameters is the same whether the receiver is in the first or second category. Beyond a certain number the quality of transmitter parameters does not improve by including more receivers in the first category. The number of receivers that belong in category (1) depends on the global distribution. Although it is currently about 35–40, that number may increase as permanently operating receivers come on-line in currently isolated regions.

Current interest in GPS geodesy is the densification of the terrestrial reference frame [*Zumberge and Liu*, 1994]. A common view, in our opinion erroneous, is that the ability to process GPS data from hundreds or thousands of receivers every day, using economical computers, is beyond the capability of any single analysis center. With the technique described here, approximately 10^3 sites can be processed with a single 40-Mflop computer every day. All solutions derived from a set of fixed transmitter parameters are in the same reference frame, which is the reference frame of the global solution from which the transmitter parameters were determined. We expect that the efficacy of the technique will be demonstrated in the dense GPS arrays in Japan and southern California.

It has long been recognized that precise GPS orbits, such as those produced by analysis centers in the IGS, improve the quality of GPS analysis. However, the value of precise GPS clocks has not been widely recognized. As we have shown, together with precise orbits, they allow analysis of data from one receiver at a time with few-millimeter daily precision in horizontal components and centimeter precision in the vertical.

Acknowledgments. We thank the Associate Editor and referees for their useful comments and criticisms. The global network of precision GPS receivers is the result of international collaboration among many groups. The authors are grateful for the rich data set that this network provides. This work was performed at the Jet Propulsion Laboratory, California Institute of Technology, under contract with the National Aeronautics and Space Administration.

References

Argus, D. F., and M. B. Heflin, Plate motion and crustal deformation estimated with geodetic data from the Global Positioning System, *Geophys. Res. Lett., 22 (15)*, 1973-1976, 1995.

Bar-Sever, Y. E., W. I. Bertiger, E. S. Davis, and J. A. Anselmi, Fixing the GPS Bad Attitude: Modeling GPS Satellite Yaw During Eclipse Seasons, *Navigation, 43 (1)*, 1996.

Bierman, G. J., *Factorization Methods for Discrete Sequential Estimation*, Academic, San Diego, Calif., 1977.

Blewitt, G., Carrier phase ambiguity resolution for the Global Positioning System applied to geodetic baselines up to 2000 km, *J. Geophys. Res., 94* 10,187-10,283, 1989.

Blewitt, G., M. B. Heflin, F. H. Webb, U. J. Lindqwister, and R. P. Malla, Global coordinates with centimeter accuracy in the international terrestrial reference frame using GPS, *Geophys. Res. Lett., 19 (9)*, 853-856, 1992.

Blewitt, G., M. B. Heflin, K. J. Hurst, D. C. Jefferson, F. H. Webb, and J. F. Zumberge, Absolute far-field displacements from the 28 June 1992 Landers earthquake sequence, *Nature, 361*, 340-342, 1993.

Blewitt, G., Advances in Global Positioning System Technology for Geodynamics Investigations: 1978-1992, in *Contributions of Space Geodesy to Geodynamics Technology, Geodyn. Ser.*, vol. 25, edited by D. E. Smith and D. L. Turcotte, pp. 195-213, AGU, Washington, D. C., 1993.

Bock, Y., et al., Detection of crustal deformation from the Landers earthquake sequence using continuous geodetic measurements, *Nature, 361*, 337-340, 1993.

Boucher, C., Z. Altamimi, and L. Duhem, *Results and analysis of the ITRF93, IERS Tech. Note 18*, Obs. de Paris, Paris, Oct., 1994.

Businger, S., S. R. Chiswell, M. Bevis, J. Duan, R. A. Anthes, C. Rocken, R. H. Ware, M. Exner, T. VanHove, and F. S. Solheim, The promise of GPS in atmospheric monitoring, *Bull. Am. Meterol. Soc., 77 (1)*, 1996.

Feigl, Kurt L., et al., Space geodetic measurement of crustal deformation in central and southern California, 1984-1992, *J. Geophys. Res., 98*, 21,677–21,712, 1993.

Gendt, G., G. Dick, and Ch. Reigber, IGS Analysis Center at GFZ Potsdam, in *International GPS Service for Geodynamics 1994 Annual Report*, edited by J. F. Zumberge, R. Liu, and R. E. Neilan, JPL Publication 95-18, Pasadena, Calif., 1995.

Heflin, M., et al., Global geodesy using GPS without fiducial sites, *Geophys. Res. Lett., 19 (2)*, 131-134, 1992.

Herring, T. A., D. Dong and R. W. King, Sub-milliarcsecond determination of pole position using Global Positioning System data, *Geophys. Res. Lett., 18 (10)*, 1893-1896, 1991.

Kouba, J., Analysis coordinator report, in *International GPS Service for Geodynamics 1994 Annual Report*, edited by J. F. Zumberge, R. Liu, and R. E. Neilan, JPL Publication 95-18, Pasadena, Calif., 1995.

Kuang, D., B. E. Schutz, and M. M. Watkins, On the structure of geometric positioning information in GPS measurements, *J. Geodesy, 71 (1)*, 35-43, 1997.

Larson, K. M., and J. Freymueller, Relative motions of the Australian, Pacific and Antarctic plates estimated by the

Global Positioning System, *Geophys. Res. Lett., 22 (1)*, 37-40, 1995.

Lichten, S. M., Estimation and filtering for high-precision GPS positioning applications, *Manuscr. Geod., 15*, 159-176, 1990.

Lindqwister, U. J., A. P. Freedman, and G. Blewitt, Daily estimates of the Earth's pole position with the Global Positioning System, *Geophys. Res. Lett., 19 (9)*, 845-848, 1992.

Melbourne, W. G., Sounding the Earth's atmosphere and ionosphere with GPS, *Eos AGU Trans., 76 (46)*, 465-466, 1995.

Noll, C. E., CDDIS Global Data Center report, in *International GPS Service for Geodynamics 1994 Annual Report*, edited by J. F. Zumberge, R. Liu, and R. E. Neilan, JPL Publication 95-18, Pasadena, Calif., 1995.

Webb, F. H., M. Bursik, T. Dixon, F. Farina, G. Marshall, and R. S. Stein, Inflation of Long Valley Caldera from one year of continuous GPS observations, *Geophys. Res. Lett., 22 (3)*, 195-198, 1995.

Wilson, B. D. , A. J. Mannucci, C. D. Edwards, Subdaily northern hemisphere ionospheric maps using an extensive network of GPS receivers, *Radio Sci., 30*, 639-648, 1995.

Wu, J. T., Estimation of clock errors in a GPS based tracking system, paper presented at the Am. Inst. of Aeronaut. and Astronaut./Am. Astronaut. Soc. Astrodynamics Conference, AIAA, Seattle, Wash., 1984.

Wu, J. T., S. C. Wu, G. A. Hajj, W. I. Bertiger, and S. M. Lichten, Effects of antenna orientation on GPS carrier phase, *Manuscr. Geod., 18*, 91-98, 1993.

Yunck, T. P., GPS data, acquisition, environmental effects, *U.S. Natl. Rep. Int. Union Geod. Geophys., 1991-1994, Rev. Geophys., 33*, 349-352, 1995.

Zumberge, J. F., and R. Liu (Eds), *Densification of the IERS Terrestrial Reference Frame Through Regional GPS Networks*, JPL Publication 95-11, Pasadena, Calif., 1994.

Zumberge, J. F., M. B. Heflin, D. C. Jefferson, M. M. Watkins, and F. H. Webb, Jet Propulsion Laboratory IGS Analysis Center 1994 annual report, in *International GPS Service for Geodynamics 1994 Annual Report*, edited by J. F. Zumberge, R. Liu, and R. E. Neilan, JPL Publication 95-18, Pasadena, Calif., 1995.

Zumberge, J. F., and W. I. Bertiger, Ephemeris and Clock Navigation Message Accuracy, in *Global Positioning System - Theory and Applications, vol. I*, edited by B. W. Parkinson and J. J. Spilker, 585-599, Am. Inst. of Aeronautics and Astronautics, Inc., Washington, D. C., 1996.

M. B. Heflin, D. C. Jefferson, M. M. Watkins, F. H. Webb, and J. F. Zumberge, Jet Propulsion Laboratory, California Institute of Technology, MS 238-600, 4800 Oak Grove Drive, Pasadena, CA 91109-8099. (e-mail: mbh@cobra.jpl.nasa.gov, djeff@cobra.jpl.nasa.gov, mmw@cobra.jpl.nasa.gov, fhw@cobra.jpl.nasa.gov, jfz@cobra.jpl.nasa.gov)

(Received May 3, 1996; revised December 2, 1996; accepted December 9, 1996.)